Original article
UDC 54.057
DOI: https://doi.org/10.18721/JPM.19211

STRUCTURAL PROPERTIES OF SOME NANOCRYSTALLINE SPINEL CHROMITES PREPARED BY SOLID-STATE REACTION METHOD

R. Yousef [1], A. Yousef [2], A. Nassif [3] ✉, Sh. A. Kadhim [4]

[1] Homs University, Homs, Syrian Arab Republic;
[2] Al-Hawash Private University, Homs, Syrian Arab Republic;
[3] Al-Wataniya Private University, Hama, Syrian Arab Republic;
[4] University of Kufa, An Najaf, Republic of Iraq
✉ nassifalaa85@gmail.com

Abstract. Chromium nanocomposites MCr_2O_4 have been synthesized by a solid-state reaction. The synthesized samples were characterized using X-ray powder diffraction technology (XRD). The temperature of synthesis was 1000°C for $NiCr_2O_4$ and 900°C for Zn Cr_2O_4. Miller indices (*hkl*) were calculated for the production, and the compounds were shown to have cubic structure FCC. The lattice parameters were as follows: $a = 8.26$ Å, $Z = 8$, $V = 564.26$Å^3 and $a = 8.2650$ Å, $Z = 8$, $V = 564.58$ Å^3 for $NiCr_2O_4$ and $ZnCr_2O_4$ respectively. The space group of symmetry is F*d*3*m* for the both. The grain sizes were calculated by the Debye − Scherrer formula for the two compounds and were 31.92 nm and 32.78 nm, respectively. The $ZnCr_2O_4$ and $NiCr_2O_4$ nanoparticles' morphology was examined using scanning electron microscopy (SEM). The SEM images showed the agglomeration of the nanoparticles, which were formed of square-shaped nanocrystallites.

Keywords: MCr_2O_4, spinel, solid-state reaction method, grain size

For citation: Nassif A., Yousef R., Yousef A., Kadhim Sh. A., Structural properties of some nanocrystalline spinel chromites prepared by solid-state reaction method, St. Petersburg State Polytechnical University Journal. Physics and Mathematics. 19 (2) (2026) 136–146. DOI: https://doi.org/10.18721/JPM.19211

This is an open access article under the CC BY-NC 4.0 license (https://creativecommons.org/licenses/by-nc/4.0/)

Научная статья
УДК 54.057
DOI: https://doi.org/10.18721/JPM.19211

СТРУКТУРНЫЕ СВОЙСТВА ДВУХ НАНОКРИСТАЛЛИЧЕСКИХ ХРОМШПИНЕЛЕЙ, ПОЛУЧЕННЫХ МЕТОДОМ ТВЕРДОФАЗНЫХ РЕАКЦИЙ

Р. Юсеф [1], А. Юсеф [2], А. Нассиф [3] ✉, Ш. А. Кадхим [4]

[1] Университет Хомса, г. Хомс, Сирийская Арабская Республика;
[2] Частный университет Аль-Хаваш, г. Хомс, Сирийская Арабская Республика;
[3] Частный университет Аль-Ватания, г. Хама, Сирийская Арабская Республика;
[4] Университет Куфы, г. Эн-Наджаф, Республика Ирак
✉ nassifalaa85@gmail.com

Аннотация. В работе были синтезированы нанокомпозиты хрома MCr_2O_4 методом твердофазных реакций. Значения температуры синтеза составили 1000°C для $NiCr_2O_4$ и 900°C для Zn Cr_2O_4. Были рассчитаны индексы Миллера (*hkl*) и показано, что соединения обладают гранецентрированной кубической структурой. Параметры решетки составили: $a = 8{,}26$ Å, $Z = 8$, $V = 564{,}26$ Å ($NiCr_2O_4$) и $a = 8{,}2650$ Å, $Z = 8$, $V = 564{,}58$ Å^3 ($ZnCr_2O_4$).

© Yousef R., Yousef A., Nassif A., Kadhim Sh. A., 2026. Published by Peter the Great St. Petersburg Polytechnic University.

Для обоих хромитов пространственная группа симметрии – F*d*3*m*. Размеры зерен, рассчитанные по формуле Дебая – Шеррера, составили 31,92 нм ($NiCr_2O_4$) и 32,78 нм ($ZnCr_2O_4$). Морфология наночастиц двух синтезированных хромитов была изучена с помощью сканирующей электронной микроскопии. На полученных изображениях была видна агломерация наночастиц, состоящая из квадратных нанокристаллитов.

Ключевые слова: MCr_2O_4, шпинель, метод твердофазных реакций, размер зерна

Для цитирования: Нассиф А., Юсеф Р., Юсеф А., Кадхим Ш. А. Структурные свойства двух нанокристаллических хромшпинелей, полученных методом твердофазной реакции // Научно-технические ведомости СПбГПУ. Физико-математические науки. 2026. Т. 19. № 2. С. 136–146. DOI: https://doi.org/10.18721/JPM.19211

Статья открытого доступа, распространяемая по лицензии CC BY-NC 4.0 (https://creativecommons.org/licenses/by-nc/4.0/)

Introduction

Mixed oxides of chromium with transition metals MCr_2O_4 where M = Ni, Zn, having a spinel structure [1], have attracted a lot of attention due to their great importance in many technical fields and their desirable industrial properties such as their high melting point, high resistance to acids and alkalis, high activity, and low production cost [2]. In recent years this fact has prompted researchers to improve and develop methods for synthesizing these materials. It is possible that the most common method for obtaining these oxides is the solid-state reaction [3], which depends on mechanical mixing of solid oxides and annealing them, in addition to many other chemical techniques that allow obtaining nanometer materials with a high degree of purity and greater homogeneity. Among them, such as the sol-gel method [2], the hydrothermal synthesis method [4], the co-precipitation method [5], and the combustion reaction method [6] are widely used.

In this research, the solid-state reaction method was adopted to synthesize a chromite – transition metal system, as the transition metal chromite has distinctive magnetic properties and is used as a catalyst in many reactions and is also used in the manufacture of gas sensors [6 – 9]. The solid-state reaction method is one of the most important ones for obtaining these compounds because of its ease of preparation, as it does not require special skills. Since some materials are difficult to dissolve in water, this method provides a solution to this problem in terms of preparing the desired compounds without the need to dissolve them in any solution. On the other hand, this advantage constitutes a high economic feasibility for the solid-state method, as the only material used in most of its reactions is acetone, which is used to facilitate the mixing of the solid compounds during the sample preparation process and in relatively small quantities.

This method is characterized by giving a high-purity mixture of what it requires of high-purity oxides without any impurities from different materials for synthesis when mixing compared to other synthesis methods. Stoichiometric ratios of the raw materials are taken in their pure form to ensure the completion of the reaction and obtain a single phase of the new pure material without the presence of other phases of impurities or raw materials [10, 11].

Experimental part

The samples of nickel chromite and zinc chromite were prepared by the solid-state reaction (SSR) method as powders by mixing appropriate amounts of nickel, zinc and chromium oxides $NiO : Cr_2O_3 = 1 : 1$ and $ZnO : Cr_2O_3 = 1 : 1$ in the presence of air. The primary nano oxides were ZnO (99% VWR International Ltd.), NiO (99% Chem-Lab.), and Cr_2O_3 (99.1% Genral Purpose Reagent). The chemical reactions between these oxides were as follows:

$$NiO + Cr_2O_3 \rightarrow NiCr_2O_4, \quad (1)$$

$$ZnO + Cr_2O_3 \rightarrow ZnCr_2O_4. \quad (2)$$

The previous materials were ground and mixed using an agate mortar to ensure obtaining a homogeneous mixture after adding an amount of acetone to improve the homogeneous mixing

© Юсеф Р., Юсеф А., Нассиф А., Кадхим Ш. А., 2026. Издатель: Санкт-Петербургский политехнический университет Петра Великого.

Table 1

The calculated masses of raw materials (oxides) used in the preparation of 10 g of each chromite

Oxide	*M*, g/mol	*m*, g
NiO : Cr_2O_3 = 1 : 1 (see Eq. (1))		
NiO	74.71	3.2951
Cr_2O_3	151.99	6.7048
ZnO : Cr_2O_3 = 1 : 1 (see Eq. (2))		
ZnO	81.37	3.487
Cr_2O_3	151.99	6.513
Cromites		
$NiCr_2O_4$	226.645	9.9999
$ZnCr_2O_4$	233.332	10.0000

Notations: *M*, *m* are respectively the molar mass and mass.

process for approximately 15 min until the acetone dried. This process was repeated three times in succession for each sample. After that, the resulting mixture was dried by heating it to a temperature of 100°C for a sufficient period of time to ensure the elimination of moisture. The raw materials' masses were calculated according to Eqs. (1) and (2) and are presented in Table 1. The required masses were estimated to get a 10 g amount of the resulting compound.

Subsequently, the powder was put inside a porcelain crucible and heated at various temperatures within the range from 600 to 1100°C for nickel chromite and from 600 to 900°C for zinc chromite. Six hours passed throughout the annealing process. After the preparation of zinc- and nickel-chromite nanoparticles the powder was compressed using a hydraulic press to create pellets with a radius of 0.5 cm and a thickness of 0.2 cm under a pressure of 10 t/m^2. The pressing process increased the interaction between the particles by bringing them closer to one another.

Results and discussion

X-ray diffraction (XRD) analysis. The prepared samples were characterised by the X-ray diffraction (XRD) technique (Philips-PW-1840, $\lambda_{CoK\alpha}$ = 1.7889 Å). By XRD technique the optimum temperature for synthesis was determined, which was the temperature that indicated the appearance of a single phase, i.e. obtaining the desired compound. In this investigation, it was 1000°C for the nickel chromite compound and 900°C for the zinc chromite compound, at which a single compound was obtained and all diffraction peaks indicated the raw materials NiO, ZnO, Cr_2O_3 being absent.

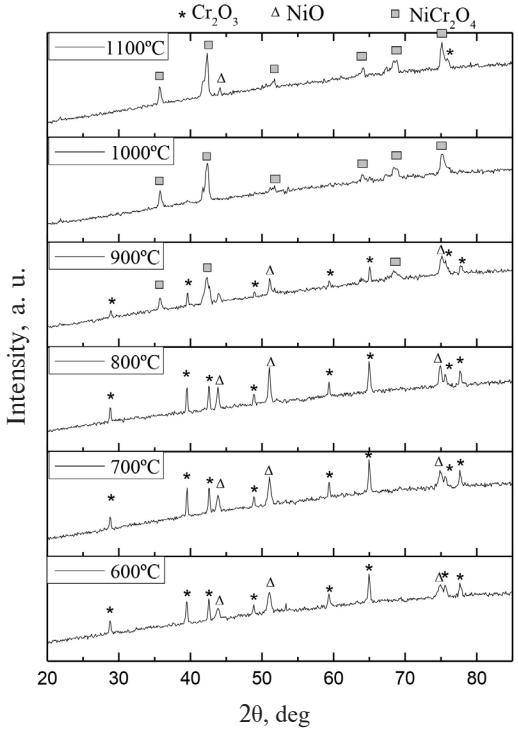


Fig. 1. XRD patterns of the prepared nickel chromite annealed at different temperatures for six hours

The scanning process was carried out using angles within the range 2θ = (20 − 85)° with an angle step of 0.02° and a time step of 2 s. The same angular range was used for all scanning processes. For the measurement procedure, the powder samples were placed on special substrates to eliminate background radiation, while the pellet samples were placed directly on the sample holder, aligned correctly with the substrate used for the powder. After collecting the diffraction data (peak positions and their intensities), the intensity values were plotted against the Bragg diffraction angle 2θ. The crystal lattice constants were then calculated from the positions of the characteristic peaks of the compound.

Nickel chromite $NiCr_2O_4$. Fig. 1 shows the XRD patterns of $NiCr_2O_4$ samples which were annealed in the temperature range from 600°C to 1100°C for 6 hrs. This data exhibited that the initial annealing process did not lead to any reaction between the raw materials, as the resulting peaks indicated a mixture of raw materials, and there was no peak indicating the desired compound.

Therefore, 600ºC could not be considered an optimum temperature for the synthesis of nickel chromite compound, and the resulting mixture was the one of thermally uncombined primary oxides only. For this reason, we gradually raised the annealing temperature while monitoring the synthesis through the resulting pattern, and we found that the primary oxides did not react with each other at all, and the peaks' locations or their intensities did not change until 900ºC. At this temperature, we noticed a clear decrease in the intensities of the peaks that were due to the raw materials, but they did not disappear, in addition to the appearance of three new peaks indicating the nickel chromite compound at the angles 2θ = 35.6º, 42.2º, 68.3º which prompted us to raise the annealing temperature to 1000ºC to ensure that the synthesis was completed perfectly at this temperature or higher temperatures were required to obtain better results. When the resulting compound was annealed at 1000ºC, we noticed that the peaks due to the primary oxides disappeared completely and that all intensive diffraction peaks were attributed to the $NiCr_2O_4$ compound. Therefore, it could be considered that a pure phase of the $NiCr_2O_4$ compound was obtained that did not contain any intermediate phases or any phases of the starting materials from which the synthesis process was finished at 1000ºC. When the annealing temperature was raised to 1100ºC, we noticed the appearance of some peaks due to the starting materials again. Consequently, it became clear to us that the $NiCr_2O_4$ compound began to decompose at 1100ºC and that 1000ºC was the optimal temperature for the synthesis of the $NiCr_2O_4$ compound. The result we reached is consistent with the published practical work [12].

All the diffraction peaks were indexed and compared with the standard JCPDS, ICSD data of the starting NiO, Cr_2O_3 oxides and $NiCr_2O_4$ compound of the numbers 04-0835, 38-1479 and 23-1271 respectively. Fig. 2 shows the XRD pattern of $NiCr_2O_4$, which was annealed at 1000ºC for 6 hrs because that was the optimal temperature for $NiCr_2O_4$ compound synthesis.

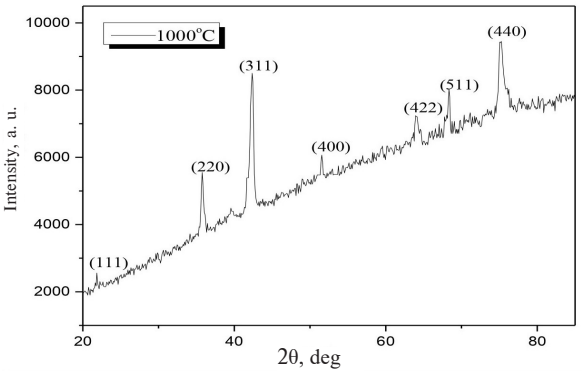


Fig. 2. XRD patterns of the prepared nickel chromite $NiCr_2O_4$ annealed at 1000°C for six hours

Miller indices of diffraction peaks were determined for the $NiCr_2O_4$ compound. These peaks indicate that the $NiCr_2O_4$ has a cubic structure and belongs to the F*d*3*m* space group. From X-ray diffraction measurements of $NiCr_2O_4$, the distance between crystal lattices *d* were calculated using the Bragg law [12]:

$$n\lambda = 2d\cdot\sin\theta,$$

where λ = 1.7889 Å is the X-ray wavelength and θ is the diffraction angle.

Then the values of the lattice constant were determined using the relation of the distance between parallel crystal plans in the case of the cubic crystal structure that is given by the formula [14]:

$$(d_{hkl})^2 = a^2/(h^2 + k^2 + l^2), \qquad (3)$$

where *a* is the lattice constant.

The values of the distance between parallel crystal plans and the lattice constant of $NiCr_2O_4$ for each diffracting peak are listed in Table 2.

An analysis of the data in Table 2 allows us to conclude that the peaks belonging to the Miller indexes (400), (311), (220) are the most intensive, and we find that they meet the conditions:

$$h + k = 2k,\ k + l = 2n,\ h + l = 2n.$$

Table 2

The results of X-ray diffraction (XRD) analysis for $NiCr_2O_4$ compound annealed at 1000ºC

2θ, dg	I/I_0, %	d_{hkl}, Å	*a*, Å	(*hkl*)
35.668	55	2.919	8.256	(220)
42.210	100	2.483	8.234	(311)
51.380	22	2.062	8.249	(400)
63.901	22	1.689	8.276	(422)
68.363	35	1.591	8.268	(511)
75.122	50	1.467	8.296	(440)

Notations: I/I_0 is the normalized intensity of diffraction peaks, d_{hkl} is the interplanar distance, *a* is the lattice constant, (*hkl*) are the Miller indices

That is, the basic cell is face-centered and therefore the compound crystallizes in Face-Centered Cubic (FCC) type. The average lattice constant of $NiCr_2O_4$ is presented in Table 3. The unit cell volume was also calculated by the following formula:

$$V = a^3 \quad (4)$$

and given in Table 3.

Table 3

Additional structural data for $NiCr_2O_4$ compound

a, Å	V, Å^3	ρ, g/cm^3		Z
		Theoretical	Experimental	
8.2634	564.26	5.3006	5.331	8

Notations: a is the average value of the lattice constant, V is the unit cell volume, ρ is the compound density, Z is the number of formulae in the unit cell.

The experimental density ρ_{exp} of $NiCr_2O_4$ was measured by the pycnometer method (distilled water was used for immersion; its density was 0.99705 g/cm^3 at 25°C). To ensure reproducibility of the results, we repeated each measurement at least 3 times for each sample. The average value is given in Table 3. The theoretical X-ray density for prepared nickel chromite was calculated as follows [11]:

$$\rho_{th} = ZM/N_A V, \quad (5)$$

where Z is the number of formula units in the unit cell ($Z = 8$ for the spinel lattice), M is the molecular mass of the nickel chromite, N_A is the Avogadro number, V is the unit cell volume.

Regarding $Z = 8$, we can write the general formula for the content of the basic cell as follows: $Ni_8Cr_{16}O_{32}$. Thus, one cell contains eight nickel atoms, sixteen chromium ones, and 32 oxygen ones. Substituting the value of Z as an integer in Eq. 5 gives us the value of the theoretical density (see Table 3). The calculated result is very close to the experimental value, which proves the accuracy of our theoretical calculations and the accuracy of our choice of the basic cell unit. The crystallite size of the $NiCr_2O_4$ compound was calculated using Scherrer's formula [14, 15]:

$$L = 0.9\lambda/(\beta \cdot \cos\theta), \quad (6)$$

where β, rad, is the full width at half-maximum (FWHM) of diffraction peaks; λ is the X-ray wavelength (λ = 1.78897); θ is the Bragg reflection angle.

The estimated values of crystallite size for each diffracting peak of $NiCr_2O_4$ compound were calculated using X'pert HighScore software and listed in Table 4. The average crystallite size was 31.92 nm, so the prepared compound had a nanostructure.

Table 4

The broadening of diffraction peaks and average grain size of $NiCr_2O_4$ compound annealed at 1000°C

Peak number	Peak position	β_{obs}	β_{std}	Grain size L, nm	
	degrees			Peak	Averaged
1	35.668	0.295	0.001	33.0	31.92
2	42.210	0.394		25.2	
3	51.380	0.295		34.8	
4	63.900			37.0	
5	68.363	0.296		37.8	
6	75.122	0.492		23.7	

Zinc chromite $ZnCr_2O_4$. Fig. 3 shows the X-ray diffraction patterns of the annealed nickel chromite compound $ZnCr_2O4$ within the temperature range from 600 to 900°C, where it appears that annealing at temperatures of 600°C to 800°C led to the formation of the zinc chromite compound, but with the presence of other peaks that refer to the raw materials, indicating that the thermal reaction is incomplete. It was found from Fig. 3 that all intensive diffraction peaks were attributed to the $ZnCr_2O_4$ compound for the sample annealed at 900°C, where the reaction between primary materials was completed. This indicates that the optimum temperature for $ZnCr_2O_4$ compound synthesis is 900°C which is lower than the temperature of nickel chromite formation.

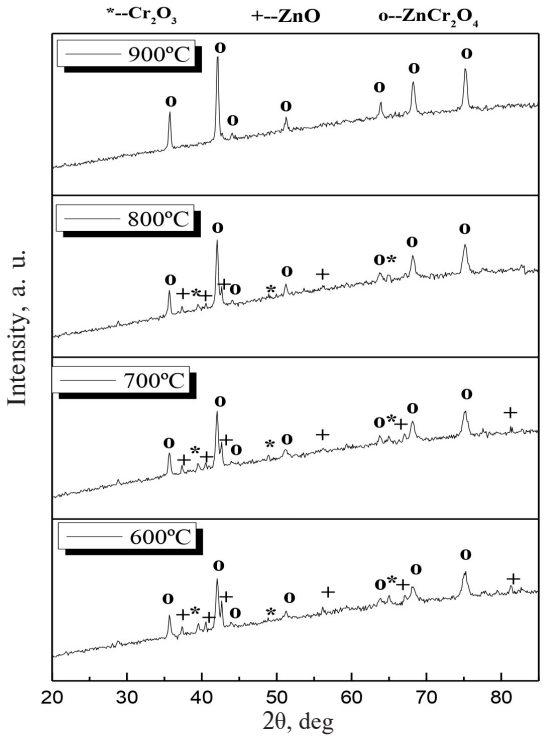


Fig. 3. XRD patterns of the prepared zinc chromite $ZnCr_2O_4$ annealed at different temperatures for six hours

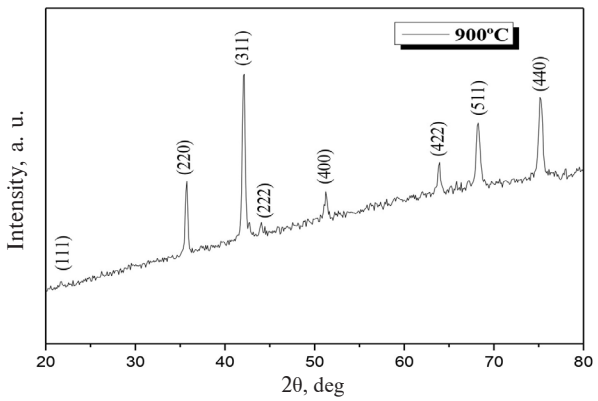


Fig. 4. XRD patterns of the prepared zinc chromite $ZnCr_2O_4$ annealed at 900°C for six hours

All the diffraction peaks were indexed and compared with the standard JCPDS, ICSD data of the starting ZnO and Cr_2O_3 oxides and $ZnCr_2O_4$ compound of the numbers 36-1451, 38-1479 and 24-495 respectively. Fig. 4 shows the XRD pattern of $ZnCr_2O_4$, which was annealed at 900 °C for 6 hrs because that is the optimal temperature for the $ZnCr_2O_4$ compound synthesis.

Miller indices of diffraction peaks were determined for $ZnCr_2O_4$ cromite. These peaks indicated that $ZnCr_2O_4$ had a cubic structure and belonged to the space group F*d3m*. From X-ray diffraction measurements of $ZnCr_2O_4$, the distance between crystal lattices and the values of the lattice constant were determined using the Bragg law and Eq. 3 for cubic crystal structure. The calculated result is listed in Table 5. The results show that the compound belongs to the cubic symmetry pattern, and all the Miller index values for all peaks agree with this crystallization pattern, which is consistent with Eq. 3.

Table 5

The results of X-ray diffraction (XRD) analysis for $ZnCr_2O_4$ compound annealed at 900°C

2θ, dg	I/I_0, %	d_{hkl}, Å	*a*, Å	(*hkl*)
21.704	6	4.7484	8.2245	(111)
35.675	45	2.9186	8.2549	(220)
42.066	100	2.4909	8.2614	(311)
44.031	7	2.3849	8.2615	(222)
51.246	16	2.0674	8.2692	(400)
63.8476	13	1.6906	8.2824	(422)
68.2505	35	1.5936	8.2804	(511)
75.2356	40	1.4646	8.2852	(440)

All notations are identical to those used in Table 2

The unit cell volume of $ZnCr_2O_4$ was calculated by Eq. 4. This value and other structural calculations such as the average lattice constant, the experimental density, the theoretical X-ray

Table 6

Additional structural data for $ZnCr_2O_4$ compound

a, Å	*V*, Å^3	ρ, g/cm^3		*Z*
		Theoretical	Experimental	
8.2650	564.58	5.49	5.45	8

All notations are identical to those used in Table 3

density, and the number of formula units in the single crystal cell are listed in Table 6. Regarding $Z = 8$, we can write the general formula for the content of the basic cell as follows: $Zn_8Cr_{16}O_{32}$. The crystallite size of the $ZnCr_2O_4$ compound was calculated using Eq. 6. The estimated values of crystallite size for each diffracting peak of $ZnCr_2O_4$ compound were calculated using X'pert HighScore software (see Table 7). The average crystallite size was 32.78 nm. Hence, the prepared compound is characterized by a nanostructure.

Table 7

The broadening of diffraction peaks and average grain size of $ZnCr_2O_4$ compound annealed at 900°C

Peak number	Peak position	β_{obs}	β_{std}	Grain size *L*, nm	
	degrees			Peak	Averaged
1	21.704	0.295	0.001	31.9	32.78
2	35.675	0.295		33.0	
3	42.066	0.295		33.6	
4	44.031			33.8	
5	51.246	0.295		34.8	
6	63.848	0.295		37.0	
7	68.251	0.394		28.4	
8	75.236	0.394		29.7	

Table 8

A comparison of the results of structural calculations for $NiCr_2O_4$ and $ZnCr_2O_4$

Compound	*a*, Å	*V*, Å^3	ρ, g/cm^3		*Z*	*L*
			Experimental	Calculated		
$NiCr_2O_4$	8.2634	564.26	5.331	5.30	8	31.92
$ZnCr_2O_4$	8.2650	564.58	5.450		8	32.78

Table 9

A comparison of our results with those obtained from literature

Compound	*a*, Å		*V*, Å^3	
	Our work	Other authors	Our work	Other authors
$NiCr_2O_4$	8.263	8.32 [17, 16]	564.26	575.96 [17, 16]
		8.27 [19, 18]		566.66 [19, 18]
$ZnCr_2O_4$	8.265	8.280 [17, 16]	564.58	567.66 [17, 16]
		8.325 [19, 18]		576.96[19, 18]

The results obtained from the previous calculations for both nickel chromite and zinc chromite compounds are arranged in Table 8. Based on those mentioned earlier, we conclude that the solid synthesis method, a straightforward and reasonably priced preparation technique, can create chromium-based spinels at temperatures between 800 and 1000°C. Furthermore, the nanoscale particle size produced by this preparation technique makes these compounds suitable for use in gas sensitivity applications, electrodes, and other fields.

Table 9 shows a comparison of the results we obtained with some other scientific works.

Scanning electron microscopy (SEM). The morphology of the $ZnCr_2O_4$ and $NiCr_2O_4$ nanoparticles was investigated using scanning electron microscopy (SEM). Fig. 5 displays the SEM images of $ZnCr_2O_4$ and $NiCr_2O_4$ nanoparticles synthesized by solid-state reactions. They show the agglomeration of the nanoparticles, which are formed up of square-shaped nanofine crystallites.

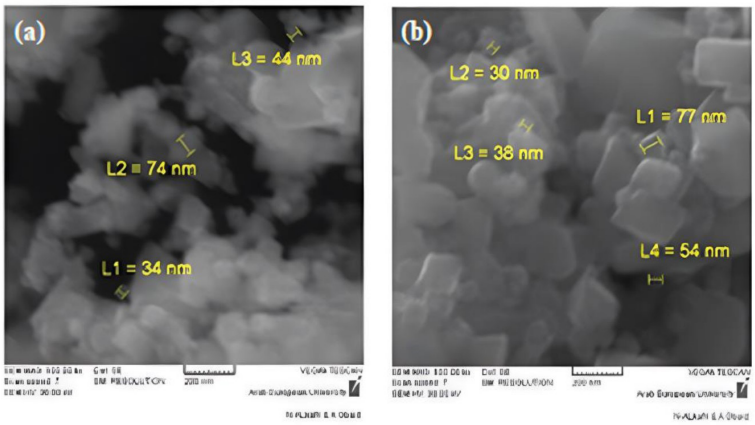


Fig. 5. SEM images of $NiCr_2O_4$ (*a*) and $ZnCr_2O_4$ (*b*) nanoparticles prepared by the solid-state method at 1000°C (*a*) and 900°C (*b*) for 6 hours

Summary

This work has shown that the straightforward and economical solid-state reaction approach can be used to synthesize nickel chromite and zinc chromite nanoparticles successfully, with the optimal synthesis temperatures of 1000°C and 900°C, respectively. Both compounds had nanoscale grain sizes of about 32 nm and crystallized in a face-centered cubic (F*d3m*) structure. The solid-state reaction approach is an effective method to create chromium-based nanocomposites since it can yield highly pure, nanostructured spinel phases at comparatively low synthesis temperatures. The produced compounds are excellent prospects for technical uses including gas sensors, electrodes, and other cutting-edge functional materials because of these structural features.

Acknowledgment

The authors would like to thank the technical team in XRD Lab at Homs University for financial support.

REFERENCES

1. **Fairooz N. Y., Imran A. R.,** Wet commixing synthesis, physical properties and photocatalytical activity of nickel oxide chromite spinel, J. Appl. Chem. 2 (Jan) (2013) 129–136.

2. **Habibi M., Fakhri F.,** Fabrication and characterization of $CuCr_2O_4$ nanocomposite by XRD, FESEM, FTIR and DRS, Synth. React. Inorg. Met.-Org. Nano-Met. Chem. 46 (6) (2016) 847–851.

3. **Ishibashi H., Yasumi T.,** Structural transition of spinel compound $NiCr_2O_4$ at ferrimagnetic transition temperature, J. Magn. Magn. Mater. 310 (2, P. 2) (2007) e610–e612.

4. **Durrani S. K., Hussain S. Z., Saeed K., et al.,** Hydrothermal synthesis and characterization of nanosized transition metal chromite spinels, Turk. J. Chem. 36 (1) (2012) 111–120.

5. **Safaei-Ghomi J., Akbarzadeh Z., Khojastehbakht-Koopaei B.,** C–N cross-coupling reaction catalysed by reusable $CuCr_2O_4$ nanoparticles under ligand-free conditions: a highly efficient synthesis of triarylamines, RSC Adv. 5 (37) (2015) 28879–28884.

6. **Abu Bakar S., Ahad N., Bin Saion E.,** Thermal treatment synthesis and characterization of nanosized nickel chromite spinels, Proc. 2012 Int. Conf. of Solid State Sci & Technol. (ICSSST-2012), Dec. 18 − 20, 2012. Holiday Inn, Malacca, Malaysia; JEOL. Serving Advanced Technology (2013) 47−54.

7. **Barros B., Costa A. C. F. M., Kiminami R. H. G. A., da Gama L.,** Preparation and characterization of spinel MCr_2O_4 (M = Zn, Co, Cu and Ni) by combustion reaction, J. Metastab. Nanocryst. Mater. 20−21 (07 Jul) (2004) 325−332.

8. **Tomiyasu K., Kagomiya I.,** Magnetic structure of $NiCr_2O_4$ studied by neutron scattering and magnetization measurements, J. Phys. Soc. Jpn. 73 (9) (2004) 2539−2542.

9. **Ptak M., Maczka M., Gągor A., et al.**, Temperature-dependent XRD, IR, magnetic, SEM and TEM studies of Jahn − Teller distorted $NiCr_2O_4$ powders, J. Solid State Chem. 201 (May) (2013) 270−279.

10. **West A. R.,** Solid state chemistry and its applications. Second edition, student edition, John Wiley & Sons, Ltd; Chichester, New York, 2022.

11. **Gao H., Guo J., Li Y., et al.,** Highly selective and sensitive xylene gas sensor fabricated from $NiO/NiCr_2O_4$ p-p nanoparticles, Sens. Actuator. B. Chem. 284 (1 Apr) (2019) 305−315.

12. **Muhammed S. A., Abbas N. K.,** Synthesis and investigation of structural and optical properties of CdO:Ag nanoparticles of various concentrations, Baghdad Sci. J. 20 (5) (2023) 32.

13. **Noshahi N. A., Nadeem K., Kamran M.,** Role of Mn doping on magnetic properties of multiferroic $NiCr_2O_4$ nanoparticles, Ceram. Int. 47 (8) (2021) 10643−10649.

14. **Bakar S. A., Soltani N., Yunus W. M. M., et al.,** Structural and paramagnetic behavior of spinel $NiCr_2O_4$ nanoparticles synthesized by thermal treatment method: Effect of calcination temperature, Solid State Commun. 192 (Aug) (2014) 15−19.

15. **Enhessari M., Salehabadi A., Khanahmadzadeh S., et al.,** Modified sol-gel processing of $NiCr_2O_4$ nanoparticles; structural analysis and optical band gap, High Temp. Mater. Process. 36 (22 Jun) (2017) 121−125.

16. **Joshi P., Saxena P., Choudhary P., et al.,** Structural and vibrational response in Al modified $NiCr_2O_4$, AIP Conf. Proc. 2100 (Apr) (2019) 020174.

17. **Yazdanbakhsh M., Khosravi I., Goharshadi E. K., Youssefi A.,** Fabrication of nanospinel $ZnCr_2O_4$ using sol-gel method and its application on removal of azo dye from aqueous solution, J. Hazard. Mater. 184 (1−3) (2010) 684−689.

18. **Kumar K. V., Bhavani S. D.,** Influence of calcination temperature on physical and optical properties of nickel chromite nanoparticles, Sci. Sinter. 54 (4) (2022) 457−468.

19. **Ghosh D., Dutta U., Haque A., et al.,** Ultra-high sensitivity of luminescent $ZnCr_2O_4$ nanoparticles toward nitroaromatic explosives sensing, Dalton Trans. 47 (14) (2018) 5011−5018.

СПИСОК ЛИТЕРАТУРЫ

1. **Fairooz N. Y., Imran A. R.** Wet commixing synthesis, physical properties and photocatalytical activity of nickel oxide chromite spinel // Journal of Applied Chemistry. 2013. Vol. 2. January. Pp. 129−136.

2. **Habibi M., Fakhri F.** Fabrication and characterization of $CuCr_2O_4$ nanocomposite by XRD, FESEM, FTIR and DRS // Synthesis and Reactivity in Inorganic, Metal-Organic and Nano-Metal Chemistry. 2016. Vol. 46. No. 6. Pp. 847−851.

3. **Ishibashi H., Yasumi T.** Structural transition of spinel compound $NiCr_2O_4$ at ferrimagnetic transition temperature // Journal of Magnetism and Magnetic Materials. 2007. Vol. 310. No. 2. Part 2. Pp. e610−e612.

4. **Durrani S. K., Hussain S. Z., Saeed K., Khan Y., Arif M., Akhmed N.** Hydrothermal synthesis and characterization of nanosized transition metal chromite spinels // Turkish Journal of Chemistry. 2012. Vol. 36. No. 1. Pp. 111−120.

5. **Safaei-Ghomi J., Akbarzadeh Z., Khojastehbakht-Koopaei B.** C−N cross-coupling reaction catalysed by reusable $CuCr_2O_4$ nanoparticles under ligand-free conditions: A highly efficient synthesis of triarylamines // RSC Advances. 2015. Vol. 5. No. 37. Pp. 28879−28884.

6. **Abu Bakar S., Ahad N., Bin Saion E.** Thermal treatment synthesis and characterization of nanosized nickel chromite spinels // Proceedings of 2012 International Conference of Solid State Sciences and Technology (ICSSST-2012). December 18 – 20, 2012. Holiday Inn, Malacca, Malaysia. JEOL. Serving Advanced Technology. 2013. Pp. 47–54.

7. **Barros B., Costa A. C. F. M., Kiminami R. H. G. A., da Gama L.** Preparation and characterization of spinel MCr_2O_4 (M = Zn, Co, Cu and Ni) by combustion reaction // Journal of Metastable and Nanocrystalline Materials. 2004. Vol. 20–21. 07 July. Pp. 325–332.

8. **Tomiyasu K., Kagomiya I.** Magnetic structure of $NiCr_2O_4$ studied by neutron scattering and magnetization measurements // Journal of the Physical Society of Japan. 2004. Vol. 73. No. 9. 2539–2542.

9. **Ptak M., Maczka M., Gągor A., Pikul A., Macalik L., Hanuza J.** Temperature-dependent XRD, IR, magnetic, SEM and TEM studies of Jahn – Teller distorted $NiCr_2O_4$ powders // Journal of Solid State Chemistry. 2013. Vol. 201. May. Pp. 270–279.

10. **Вест А.** Химия твердого тела. Теория и приложения. В 2-х ч. Пер. с англ. М.: Мир, 1988. Ч. 1 – 558 с. Ч. 2 – 334 с.

11. **Gao H., Guo J., Li Y., et al.** Highly selective and sensitive xylene gas sensor fabricated from $NiO/NiCr_2O_4$ p-p nanoparticles // Sensors and Actuators B: Chemical. 2019. Vol. 284. 1 April. Pp. 305–315.

12. **Muhammed S. A., Abbas N. K.** Synthesis and investigation of structural and optical properties of CdO:Ag nanoparticles of various concentrations // Baghdad Science Journal. 2023. Vol. 20. No. 5. P. 32.

13. **Noshahi N. A., Nadeem K., Kamran M.** Role of Mn doping on magnetic properties of multiferroic $NiCr_2O_4$ nanoparticles // Ceramics International. 2021. Vol. 47. No. 8. Pp. 10643–10649.

14. **Bakar S. A., Soltani N., Yunus W. M. M., Saion E., Bahrami A.** Structural and paramagnetic behavior of spinel $NiCr_2O_4$ nanoparticles synthesized by thermal treatment method: Effect of calcination temperature // Solid State Communications. 2014. Vol. 192. August. Pp. 15–19.

15. **Enhessari M., Salehabadi A., Khanahmadzadeh S., Arkat K., Nouri J.** Modified sol-gel processing of $NiCr_2O_4$ nanoparticles; structural analysis and optical band gap // High Temperature Materials and Processes. 2017. Vol. 36. 22 June. Pp. 121–125.

16. **Joshi P., Saxena P., Choudhary P., Varshney M. D., Mishra A.** Structural and vibrational response in Al modified $NiCr_2O_4$ // AIP Conference Proceedings. 2019. Vol. 2100. No. 1. April. P. 020174.

17. **Yazdanbakhsh M., Khosravi I., Goharshadi E. K., Youssefi A.** Fabrication of nanospinel $ZnCr_2O_4$ using sol-gel method and its application on removal of azo dye from aqueous solution // Journal of Hazardous Materials. 2010. Vol. 184. No. 1–3. Pp. 684–689.

18. **Kumar K. V., Bhavani S. D.** Influence of calcination temperature on physical and optical properties of nickel chromite nanoparticles // Science of Sintering. 2022. Vol. 54. No. 4. Pp. 457–468.

19. **Ghosh D., Dutta U., Haque A., Mordvinova N. E., Lebedev O. I., Pal K., Gayen A., Seikh M. M., Mahata P.** Ultra-high sensitivity of luminescent $ZnCr_2O_4$ nanoparticles toward nitroaromatic explosives sensing // Dalton Transactions. 2018. Vol. 47. No. 14. Pp. 5011–5018.

THE AUTHORS

YOUSEF Rasha
Homs University
PP75+5VC, Damascus – Aleppo Highway, Homs, Syrian Arab Republic
ryousef@homs-univ.edu.sy

YOUSEF Areej
Al-Hawash Private University
Q8HJ+RMH, Al-Mouzeina, Homs, Syrian Arab Republic
areejyousef@hpu.edu.sy

NASSIF Alaa
Al-Wataniya Private University
XQ92+PMC, Hama, Syrian Arab Republic
nassifalaa85@gmail.com
ORCID: 0000-0001-6190-4642

KADHIM Shaymaa Awad
University of Kufa
P.O. Box 21, Kufa, Najaf Governorate, 540011, Republic of Iraq
shaymaa.alshebly@uokufa.edu.iq
ORCID: 0000-0002-3991-5318

СВЕДЕНИЯ ОБ АВТОРАХ

ЮСЕФ Раша – *PhD в области физики конденсированного состояния, преподаватель Университета Хомса, г. Хомс, Сирийская Арабская Республика.*
PP75+5VC, Syrian Arab Republic, Homs, Damascus – Aleppo Highway, Homs University
ryousef@homs-univ.edu.sy

ЮСЕФ Аридж – *PhD, преподаватель Частного университета Аль-Хаваш, г. Хомс, Сирийская Арабская Республика.*
Q8HJ+RMH, Syrian Arab Republic, Homs, Al-Mouzeina, Al-Hawash University
areejyousef@hpu.edu.sy

НАССИФ Алаа – *доктор военных наук, профессор инженерного факультета Частного университета Аль-Ватания, г. Хама, Сирийская Арабская Республика.*
XQ92+PMC, Syrian Arab Republic, Hama, Al-Wataniya Private University
nassifalaa85@gmail.com
ORCID: 0000-0001-6190-4642

КАДХИМ Шаймаа Авад – *PhD, профессор кафедры физики Университета Куфы, г. Эн-Наджаф, Республика Ирак.*
P.O. Box 21, Republic of Iraq, Kufa, Najaf Governorate, 540011, Kufa University
shaymaa.alshebly@uokufa.edu.iq
ORCID: 0000-0002-3991-5318

Received 30.09.2025. Approved after reviewing 08.12.2025. Accepted 08.12.2025.
Статья поступила в редакцию 30.09.2025. Одобрена после рецензирования 08.12.2025. Принята 08.12.2025.

© Санкт-Петербургский политехнический университет Петра Великого, 2026